Efficacy of Densitometric and Multispectral Techniques for Monitoring Infestations of Citrus Snow Scale on Citrus Bark

L. I. Terry
Department of Entomology, University of Arizona, Tucson, AZ 85721
G. J. Edwards
AREC, University of Florida, Lake Alfred, FL 33850

ABSTRACT: Insecticides and parasites released for control of citrus snow scale (CSS [*Unaspis citri* (Comstock); (Insecta:Homoptera)] must be routinely monitored in citrus orchards. Several analytical techniques used in aerial and multispectral photography were adapted to assess their ability to distinguish between various CSS morphs on citrus trees: males, females, and crawlers from the background, and dead from live and/or parasitized females and/or males. Film and filter combinations included black-and-white films with ultraviolet filters; black-and-white infrared film with interference and long bandpass filters; and color infrared and reversal film. Males and crawlers were easily distinguished under most scenarios. Live and dead males were separable under particular film and filter combinations, but no density differences were found between live and dead females. Photographic techniques as analyzed by densitometric or multispectral methods are not acceptable for monitoring CSS compared to more reliable and accurate visual techniques.

INTRODUCTION

CITRUS SNOW SCALE (CSS)(*Unaspis citri* (Comstock)) is a damaging pest of citrus which feeds on the phloem tissue from the trunk or leaves (Bullock and Brooks, 1975). Several life forms exist in this species: the crawler (a small, orange mobile first instar); a pre-adult white tricarinate male (immobile); adult alate male, and the sessile, brownish oyster-shaped female. Many candidate pesticides and parasites are tested for control of this insect several times per year. To evaluate these control efforts as well as to investigate life history patterns of this insect, researchers must spend tedious hours plucking each scale from the bark and examining its status with the aid of a 10x hand lens. If proven realiable, photographic methods in combination with densitometric and/or multispectal analysis could save many hours in the field.

Most remote sensing applications to agricultural pest problems involve aerial photography or thermography evaluating symptoms or indirect effects rather than the pest or stress directly (Ausmus and Hilty, 1972; Ciesla *et al.*, 1971; Edwards, 1975; Hart, 1973; Hart and Myers, 1968; Heald *et al.*, 1972; Jackson *et al.*, 1974; Marks *et al.*, 1974). Because the stress from CSS may build gradually and the stress differential between this and other potential stresses may be small, the accuracy of measuring CSS (or a symptom induced by CSS damage) by aerial means may be limited. Therefore, photographic procedures were tested directly on the insect from trunks of trees. Scenes from trunks, photographed with a 35-mm camera with many films and filters, were analyzed visually and by densitometric and multispectral image analyzers. If any combination of techniques and analytical methods proved successful at separating critical morphological forms, then techniques would be modified to improve the cost effectiveness and efficiency of the method.

PROCEDURES

Determining Ranges of CSS Reflectance

To determine which spectral range (within the range of photographic films with glass lenses) might give the greatest density difference among categories of scales, continuous reflectance spectral curves from 360 to 850nm were obtained with an intergrating sphere reflectance attachment to a Beckman D K-2a Ratio Recording Spectrophotometer. Bark was tested with no scales and no algae, very light scale infestation and algae, dense infestations of males with and wihtout algae, and dense and light infestations of females with no algae. These were the most commonly found situations under field conditions.

Film and Filter Combinations

Films that were indicated by above readings to be the most useful were black-and-white high speed infrared (BWIR), Ektachrome Infrared (EIR) (ASA 100), Kodachrome 64 (K64) (ASA 64), and Tri-X Pan (ASA 400) with an ultraviolet Kodak Wratten #18-A filter. A yellow filter (Tiffen #12) was used with EIR film to prevent blue light from exposing all layers of the film. A series of second-order interference filters (Bausch and Lomb) in increments of approximately 10 nm with halfwidths of 8 to 10 nm from 590 to 690 nm and 430 and 480 nm were used to obtain details of reflectance and film exposure patterns by CSS within this range. A red filter was used with these filters to prevent harmonic wavelengths from exposing the film and to allow only the nominal wavelength to pass. All filter combinations were within 1 percent or closer to their nominal wavelength as determined by transmission curves tested on a D K-2a spectrophotometer. Two Kodak Wratten filters, #87 (800nm) and #89B (750nm) infrared filters, were used for the 700- to 850-nm region. All interference and 89B and 87 filters were used with the BWIR film only, so these could be compared when processed to the same gamma.

A Nikon-F with a 55-mm *f*/3.5 micor-Nikkor lens plus M-3 ring at 1:1 ratio was used for all photography. Two flash units were employed at a 45° angle to the subject to give even illumination as determined by tests of various light sources. Flash distances varied depending on film/filter combinations. Appropriate focal adjustments were made for photographing in the ultraviolet and infrared range.

Scenes

A series of photographs were made on each of 12 scenes (i.e., a 35- by 24-mm section of bark containing at least 150 scales). The first two scenes were completed on infested limbs brought into the laboratory, while the remainder were taken in the field. Except for scene one, BWIR film was developed in D-19 (to give

PHOTOGRAMMETRIC ENGINEERING AND REMOTE SENSING,
Vol. 55, No. 10, October 1989, pp. 1471-1475.

0099-1112/89/5510–1471$02.25/0

high gamma for a great density range) for 9 min at 19.5° C and Tri-X Pan was developed in Polydol (also high contrast) for 9 min at 19.4° C. In scene one, Microdol X, a low contrast (low gamma, small density range) developer (10 min at 22.2° C), was used. Sensitometric curves for each developer were used for determining density ranges. In each scene all film/filter combinations were used and then analyzed visually by several image analysis and enhancement techniques. Additionally, scenes 3 to 12 were compared with and without ethanol sprayed on the scales to test for image enhancement with each film type. Each method was compared to the "trunk" truth of the scene by the following methods. Individual scales were observed through either a binocular dissecting scope (scenes studied in the laboratory) or through a 10X hand lens. A representation of the image of each scale was drawn on graph paper in proportion to its size, shape, and location within the scene for each category of scale (Figure 1).

Several solvents and dyes were compared visually for their ability to enhance the image. A particular dye/solvent combination might differentially stain live and dead males or females because of active wax secretion to the outer integuments of live scales.

Human Evaluation

Slides or negatives were observed either through a binocular microscope or projected onto a screen. Each scale was compared to that represented on the trunk truth. The percent accuracy was calculated from the formula, % accuracy = [(#LC- #LNC + #DC - #DNC/maximum possible correct] x 100, where #LC = number counted as live; #LNC = number live but counted as dead; #DC = number counted as dead; #DNC = number dead but counted as live. This separates out errors of omission (not counting them as live when they are dead) and commission (counting as live when they are dead).

Image Analyzers

Slides and negatives were analyzed by densitometric and enhancement techniques on instrumentation located at the Kennedy Space Center, Florida, Data Analysis Facility in cooperation with NASA. Data from film were input into a Digicol (International Imagery Systems, Mountain View, California) system through a scanner camera. Negatives from the black-and-white (BW) films were viewed and density measurements taken. Individual scales were observed and compared within and across all negatives of each scene of the BWIR from scenes one through four. All density measurements that fell into the toe or shoulder of the sensitometric curve for the particular film and developer combination or outside the calibration range of the instrument were not used. A two-factor analysis of variance (ANOVA) model was used to determine the effects of the type of scale and the peak wavelength of each filter on the diffuse density reading.

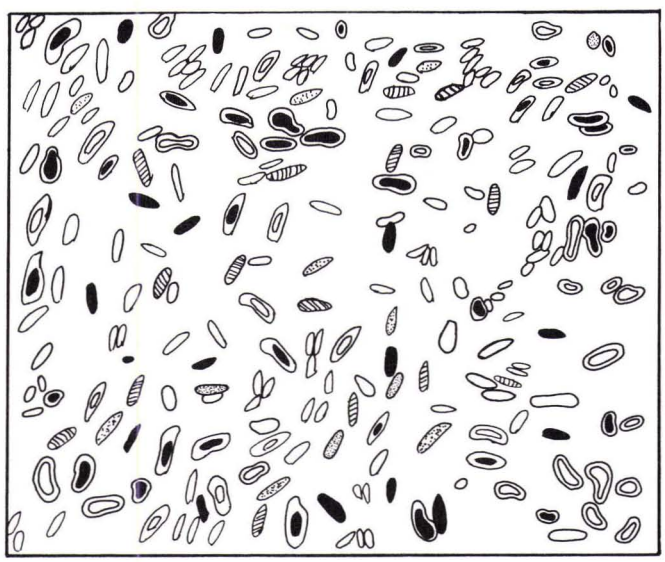

FIG. 1. A diagram of scene 3 with representative figures for each scale morph: ⬭ = dead male; ⬬ = live male; ⬭ = integument of male; ⬭ = dead male with parasite hole; ◎ = dead female; ⬬ = live female

Diffuse density was measured on BW and color negatives or slides with a P-1700 microdensitometer by scanning the film located on a rotating drum line by line, incrementing in steps of 12.5-μm diameter spots. The density information was digitized and stored on a magnetic tape and data were transformed by a series of operator controlled programs: contrast stretching, density slicing, and density stripping at each of the peak wavelengths. The resulting post-transformation images were then compared across various films/filters within the same scene.

Multiband images (color negatives from all series, and selected color IR and BWIR) were scanned at a pixel size of 50 μm by an Image 100 multispectral analyzer (General Electric) and separated into their three additive color primaries. These images were subjected to several preprocessing and postprocesng functions to search for definitive spectral signatures for each type of scale. Among the prepocessing transformations tested were ratioing and summation of channels and spectral rotations. Postprocessing functions included signature extraction of various transformed areas, theme extraction, theme synthesizing, thresholding, and clustering procedures. Single pixel training was performed on contrast streched data of two slides (ethanol treated and untreated) from scene three. First a scale of interest was located with the cursor, and a 6-by 6-pixel array of density levels around the trained object was obtained for each channel. A single pixel was selected from this array on all male scales in the scene on both slides. An ANOVA tested the effects of the independent variables of type of treatment (ethanol and no ethanol) and the type of male scale, and the variation among samples (nested within treatment and type of scale) on the diffuse density from each channel was tested. Also, averaging of a 3- by 3-pixel array within the 6- by 6-array was tested to reduce background "noise" and improve signature extraction.

RESULTS

Reflectance Curves

Reflectance curves for male and female citrus snow scale and the bark (with and without algae) all follow the same general pattern (Figure 2). All these categories reflect relatively little light in the near ultraviolet and blue portions of the spectrum and a relatively high percentage of near infrared light. This pattern is indicative of that found in most plant tissues, particularly leaf tissue, where there is an increase in reflectance in the near IR around 750 to 800 nm due to water in the cytoplasm. The bark with a light scale infestation but algae reflected at a peak of 530, the green reflectance peak, and had a much greater reflectance in the near IR. Male scales reflected the most light compared to to other categories. The greater the number of males, the higher the reflectance, whether the background was bark with or without algae. Female scales, on the other hand, reduced light reflectance when compared to the bark. There was little difference between the background (bark) and females. The region with the greatest reflectance and greatest difference in reflectance between males and females and between males and the background was around 500 to 800 nm. Films and filters sensitive in these regions were used.

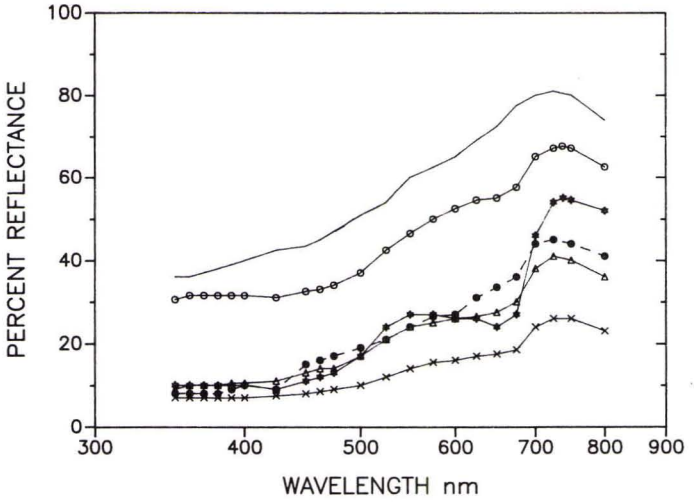

FIG. 2. DK-2a Spectrophotometer reflectance curves of citrus snow scale on citrus bark (spot diameter measured = 1.9 cm). Legend: —— bark with greatest density of male infestation, no algae; ⊶⊶ bark, dense male infestation and algae; ⊱⊰ bark, light scale infestation, algae; •—•—• bark, no scales, no algae; ⊱⟶ bark, dense female infestation, algae; ×—×—× bark, dense female infestation, no algae

TABLE 1. SOLVENTS AND DYES TESTED FOR DIFFERENTIAL STAINING OF LIVE AND DEAD MALE AND FEMALE CITRUS SNOW SCALE

		Effect on	
Dye	Solvent	Male	Female
Solvent only	Acetone	Live ones show	No difference
	Hexane	Live ones show	No difference
	70% Ethanol	Live ones show	No difference
	70% Isopropanol	Live ones show	No difference
	Water	No difference water is repelled	
Sudan IV	Hexane	Al stain pink	No difference
	Acetone	All stained pink	All stained pink
	Ethanol	All stained pink	All stained pink
	Isopropanol	All stained pink	All stained pink
	Oil	All stained bright pink	
Aniline blue	10% Ethanol	All stained blue	All stained purple
	Acetone	All stained blue	All stained purple (& background)
Eosin y	70% Isopropanol	No difference	All stained pink
	70% Ethanol	No difference	No difference
	Acetone	All stained pink	All stained slight pink (& background)

DYES AND SOLVENTS

The solvents acetone, 70 percent isopropanol, 70 percent ethanol, and hexane reduced the white reflectance of the pre-adult male integument, and the orange body of live CSS males would show through the cuticle. Ethanol only was selected to use in subsequent tests to determine the ease and accuracy of counting males scales. The solvents had no enhancement effect on the females (Table 1) as detected by human evaluation. The dyes tested had no differential staining effect on live or dead scales (Table 1) and many dyes stained only the male.

The accuracy of distinguishing live CSS males with the ethanol treatment was evaluated. Counts from ten 2.54 cm^2 treated scenes were made by plucking scales from the bark and observing scales through a 10x hand lens. Accuracies ranged from 88 to 96 percent. Dim or bad lighting proved a hindrance in making determinations. In addition to these counts, 1000 treated male scales on the trunks were determined to be either live or dead on the basis of the orange color. Errors of omission were about 7 percent and errors of commission were approximately 2 percent.

HUMAN EVALUATION OF SLIDES

In scenes 1 to 12 all the color films were analyzed by eye for accuracy of counting CSS. In all color positive slides of nontreated scenes, the total number of males, crawlers, and sometimes females were counted. Live crawlers were easily distinguished from dead crawlers. However, live males could not be distinguished from dead males on the basis of color or degree of brightness in the photograph. Live and dead female scales could not be distinguished, and many times the females could not be distinguished from the bark. Accuracy evaluations were therefore not made on the nontreated scenes by human evaluation. In the ethanol treated scenes (from 3 to 12 only) males were easily distinguished from the background. Accuracy figures, based upon live and dead male scales, ranged from 45 to 90 percent. EIR film offered no advantage in recognizing the different categories of scales either with or without the ethanol treatment. Accuracy was >98 percent for counts of male scale.

We found that counting CSS from black-and-white negatives was very difficult, whether scenes were ethanol treated or nontreated. Fine shades of grey could not be distinguished on the film. Differences in shapes, sizes, etc., did not aid the counting. Therefore, all of the black-and-white negatives were analyzed from data taken from image analysis equipment only.

IMAGE ANALYSIS TECHNIQUES

The useful density range as determined from sensitometric curves for the Infrared film with the D-19 developer was 0.15 to 1.9, with Microdol X from 0.05 to 0.85, and for Tri-X Pan with Polydol from 0.25 to 2.1.

Scenes 1 and 2 "trunk" truths included females as well as males. Female scale density data obtained by the Digicol and P-1700 Microdensitometer indicated that there were no consistent differences between either live and dead females or between females and the background. Types of male scales from scenes 1 and 2 were either dead or live pre-adult male scales. Analysis of these two types indicated that there was little difference between them. In subsequent scenes (3 to 12) which included ethanol and no ethanol treatments, four types of males were found: live pre-adult males, dead males, old integuments of males (adults had emerged), and dead males with parasite emergence holes. Crawlers were distinguished easily from the background, except when ethanol was used on the scene. Therefore, analysis efforts concentrated mainly on the recognition of the various male scale categories.

DIGICOL

Slides and negatives from scenes 1 through 12 were evaluated by the Digicol. Colors were assigned to the different categories of scales. The density levels of the females overlapped those of the background and so could not be distinguished. There was some overlap between density readings of live and dead males from negatives of both of Microdol-X developer (low contrast) and D-19 developer (high contrast).

The ANOVA model of BWIR and Tri-X film density data (at a 256 grey level resolution) indicated that there was variation among types of male scales ($F = 198$, $df = 3, 48$, $P < 0.0001$) and among wavelengths ($F > 19.1$ $df = 13,48$, $P < 0.001$) but the particular separation depended upon the peak wavelength (i.e., there were significant scale × wavelength interactions, $F = 1.7$, $df = 39,48$, $P < 0.05$) for both ethanol treated and nontreated scene. Because there were significant interactions, a Duncan's New Multiple Range Test was completed for the individual treatment combinations at $P = 0.05$ on both data sets. Results are presented as the difference among means of the different types of scales

at each wavelength (i.e., for each wavelength the different categories of scales are ranked) (Figure 3 and 4). In the nontreated scene, live males had slightly higher densities (but not significantly higher) than dead males at each wavelength except at 590, 600, 630, and 640 nm. Live male scales were not significantly different from other types at any wavelength except at 630 nm and 690 nm. The integuments of the scales were significantly different from the other categories generally, and the background had the lowest mean density reading of all categories. In the ethanol treated scene, density readings of the different categories were closer together within each wavelength (i.e., there is much greater overlap among types of scales). Live males had consistently higher mean densities over the other categories of scales, but these differences were not significant at the P = 0.05 level (Figure 4) except at 430 nm.

The information from the Tri-X/ultraviolet film/filter combination was handled separately from the infrared data because the films were developed to different gammas. There was no significant difference among types of male scale of the untreated scene. There was significant variation among types of scales from the ethanol treated scene. A Duncan's New Multiple Range Test revealed that there was no significant difference between live and dead males, although there were differences between live males and integuments of the males at the P = 0.05 level.

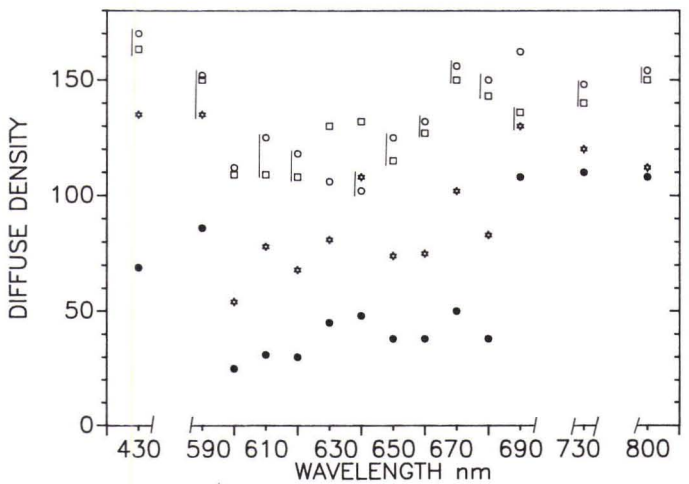

FIG. 3. Separations of male scale categories at each peak wavelength from 2nd order interference filters on Black-and-White High Speed IR film with no ethanol treatment. Legend: ○ = live male; □ = dead male; * = integument of male, ● = background

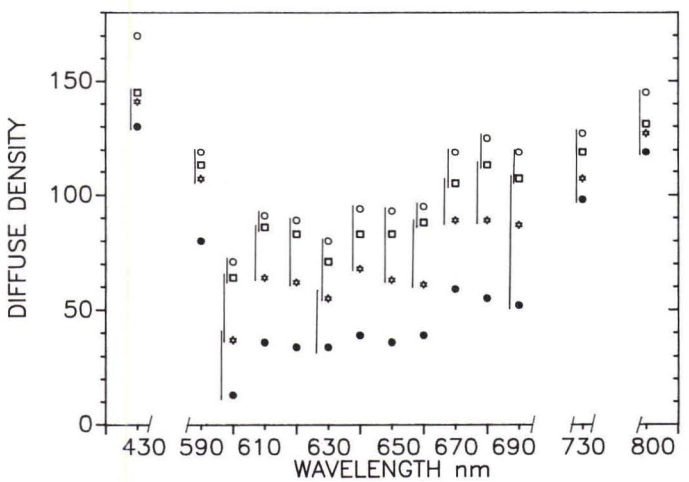

FIG. 4. Separations of male scale categories at each peak wavelength corresponding to 2nd order interference filters on Black-and-White High Speed IR film with ethanol sprayed on the scene. Legend: ○ = live male; □ = dead male; * = integument; ● = background.

Several slides as well as black-and-white negatives were analyzed by a microdensitometer instrument at a grey level resolution of 256. Raw data as well as the programmed data of scenes 1, 2, and 3 were evaluated. From scene 1, an integrated program which included a contrast stretch and density stripping eliminated all the females and the background from the entire scene. However, live males could not be separated from dead males with greater than a 50 percent accuracy from this transformed data. There was too much overlap between the two groups. Other slides and negatives of the series were also tested by these same programs, but the results were the same: female scale categories matched each other and the background, and the different types of males overlapped.

Color slides were studied by separating each slide into three color primaries: red, green, and blue. These separations were placed into channels one, two, and three of the memory of the Image 100. Because registration of black-and-white negatives was poor, only color slides were evaluated by this instrument. Four color images were chosen from scenes 1 through 12 to run through a series of programs which transformed the data from these slides to false color images. The transformed images did not yield any greater than 40 percent accuracy on the male counts. Spectral signatures could not be established exclusively for any particular category of male or female scale with the sequence of programs and transformations tested.

The results of the single pixel selection from the 6- by 6-pixel array training evaluated by an ANOVA indicated significant variation between the two treatments, among types of scales as well as among samples, for each of the three primary colors (Table 2). A Duncan's New Multiple Range Test of the variation among male scale types by treatment resulted in the following: no significant differences among the live, dead, or parasitized males, but the old integuments of males had significantly lower densities than the other categories of scales (Table 2). Similar results were obtained with the 3- by 3-array averaging technique: there were no significant differences between the live male scales and all other categories except the empty integuments.

TABLE 2. EFFECTS OF TREATMENT (ETHANOL VERSUS NO ETHANOL) AND TYPE OF MALE CITRUS SNOW SCALE ON THE DENSITY MEASURED FROM MULTISPECTRAL ANALYSES OF COLOR SLIDES (6- BY 6-PIXEL ARRAYS).

Channel color[a]	Scene treatment F		Type of male scale* F	Dead	Live	Parasitized	Integument
Red	67***	No Ethanol	7.5*	124a	122a	119a	91b
Red		Ethanol		89a	89a	84a	62b
Blue	39**	No Ethanol	4.5*	105a	104a	99a	78b
Blue		Ethanol		81a	75b	69b	56c
Green	85***	No Ethanol	5.4*	139a	133a	129a	94b
Green		Ethanol		85a	78a	73a	53b

*Those means in the same row followed by the same letter are not significantly different at the P = 0.05 level.

**Significant at P = 0.05 level, ***P = 0.0001

[a]'Treatment x type' interactions were not significant (F < 0.32, P > 0.10) for all three color channels; df for each color: treatment = 1, 488; type of scale = 3, 488; and interaction 3, 488. Sample variation (within treatment x type) was significant, (F > 32.3, df = 220, 488, P < 0.05)

DISCUSSION

CSS reflectance evaluations made by the spectrophotometer were only crude indications of the spectral regions of greatest difference in reflectance. Much finer spot sizes should be measured; ideally a spot the size of the CSS. This should yield a more accurate assessment of the differences between live and dead parasitized scales.

The evaluation of the ethanol treatment on CSS males by observation of scales through a 10x hand lens ranges from 87 to 97 percent accuracy, whereas estimations of males scales from color slides ranged from 45 to 90 percent, with an average accuracy of 82 percent. There may be several reasons for this reduction in accuracy from field observation to film. Primarily, the color slides did not truly reproduce the color of the scenes from the tree. Perhaps another film or a different processing might improve the color reproduction and consequently improve the accuracy. Secondly, many of the errors of commission might be results of those incorrectly evaluated as live but might have been parasitized males whose parasites had not yet emerged. A microscope rather than a 10x hand lens would be necessary to observe larval or pupal parasites in pre-adult male scales. Gathering this data in the field would be difficult but necessary to evaluate the effect of parasitism on the reflectance patterns.

The results of the image analysis of both black-and-white negative films and color positives revealed that there are basically few significant differences between the live and dead categories of male and female scale. Females were difficult to detect from the background. Use of an estimation procedure of the number of females by a regression on the number of males and crawlers might be incorrect in the case of differential mortality to one of the other sex. With the nontreated scene there was a significant difference between the live and dead male scales with only the 630-nm and 690-nm peak interference filters. This statistically significant difference may be useful in distinguishing live male scales by instruments, but the human eye could not separate them. Spatial pattern recognition programs might increase the accuracy of the counts. When the costs, the handling time, and the chances of losing a count are considered, the photographic methods tested here are not the most practical means for monitoring CSS on citrus.

ACKNOWLEDGMENTS

The authors would like to thank the cooperation received by the NASA engineers at Kennedy Space Center, especially Tom Davis and Joe Bartosek. Mention of a trademark or proprietary product does not constitute an endorsement of the product by the authors or their institutions and does not imply its approval to the exclusion of other products that may be suitable.

REFERENCES

Ausmus, B. S., and J. W. Hilty, 1972. Aerial detection of maize dwarf mosaic virus-diseased corn. *Phytopathology*, 62:1070–1074.

Bullock, R. C., and R. F. Brooks, 1975. Citrus pest control in the USA. *Citrus* (E. Hafliger, ed.), CIBA-GEIGY Tech. Monogr. No. 4., Basle, Switzerland, p. 35–37.

Ciesla, W. M., L. W. Drake, and D. H. Wilmore, 1971. Color photos, aerial sprays, and forest tent caterpillar. *Photogrammeteric Engineering*, 37:867–873.

Edwards G. J, 1975. Multispectral sensing of citrus Young Tree Decline. *Photogrammetric Engineering and Remote Sensing*, 41:653–657.

Hart, W. G., 1973. Aerial photography with infrared as a method for survey for citrus blackfly (Aleurocanthus woglumi). *J. Econ. Entomol.*, 66:190–194.

Hart, W. G., and V. I. Myers,. 1968. Infrared aerial color photography for detection of populations of soft scale in citrus groves. *J Econ. Entomol.*, 61:617–624.

Heald, C. M., W. H. Thames, and C. L. Wiegand, 1972. Detection of Rotylenchus reniformis infestations by aerial infrared photography. *J. Nematol.*, 4:298–300.

Jackson, H. R., V. R. Wallen, D. Galway, and S. W. MacDiarmid, 1974. Corn aphid infestation computer analyzed from aerial color-IR. *Photogrammetric Engineering*, 41:943–952.

Marks, C. F., J. M. Elliot, J. R. Rainforth, M. C. Watson, and B. Back, 1974. Aerial photography—an aid in survey for damage by rootleison nematode in fluecured tobacco. *Can. Plant Dis. Surv.*, 54:105–107.

(Received 30 August 1988; revised and accepted 9 March 1989)

BOOK REVIEWS

Satellite Monitoring of the Earth by Karl-Heinz Szekielda. John Wiley and Sons, Inc., 605 Third Avenue, New York, New York, 10158. 326 pages, 251 illustrations including 9 colored plates, Hardcover. Copyright 1988, publication date 1 February 1989, $54.95.

Satellite Monitoring of the Earth by Karl-Heinz Szekielda is designed as an introduction to remote sensing as well as a synopsis of state-of-the-art applications of remote sensing technology from space platforms for monitoring the Earth. The book is organized into seven chapters: Introduction (Chapter 1), Platforms and Sensors (Chapter 2), Atmospheric Considerations (Chapter 3), Spectral Characteristics of Natural Systems (Chapter 4), Concepts in Data Processing and Interpretation (Chapter 5), Observations Over the Oceans (Chapter 6), and Observations Over the Continents (Chapter 7).

Chapter 1 (7 pages including 3 illustrations) provides a brief description of electromagnetic radiation and the structure of the electromagnetic spectrum. Basic radiation laws and relationships are introduced and interactions between Earth materials and electromagnetic energy are briefly discussed.

Chapter 2 (48 pages including 32 illustrations and 11 tables) discusses satellite platforms and sensor systems from TIROS to NIMBUS to ITOS. The discussion continues to include satellite systems such as GOES/SMS, Landsat, and SPOT. Illustrations are provided that detail the configuration of some of the satellite platforms, communication linkages between satellites and ground receiving stations, and selected orbit characteristics. The description of satellite sensor systems that are used in assessing Earth resources are organized under primary headings: Sensors for the Visible and Near Reflected Infrared, Infrared Sensors, Microwave Sensors, and Magnetic Sensors.